# Life cycle assessment of biodiesel production utilising waste date seed oil and a novel magnetic catalyst: A circular bioeconomy approach

**Kamla S. Al-Mawali[1], Ahmed I. Osman[2*], Ala'a H. Al-Muhtaseb[1*], Neha Mehta[3], Farrukh Jamil [1,4], Farouk Mjalli[1], G. Reza Vakili-Nezhaad[1], David W. Rooney[2]**

[1] Department of Petroleum and Chemical Engineering, College of Engineering, Sultan Qaboos University, Muscat-Oman

[2] School of Chemistry and Chemical Engineering, Queen's University Belfast, Belfast BT9 5AG, Northern Ireland, UK

[3] School of Mechanical and Aerospace Engineering, Queen's University Belfast, Belfast BT7 1NN, Northern Ireland, UK

[4] Department of Chemical Engineering, COMSATS University Islamabad, Lahore Pakistan

Corresponding Authors:

Dr. Ahmed I. Osman

Email: aosmanahmed01@qub.ac.uk

Dr. Ala'a H. Al-Muhtaseb

Email: muhtaseb@squ.edu.om

**Graphical abstract**

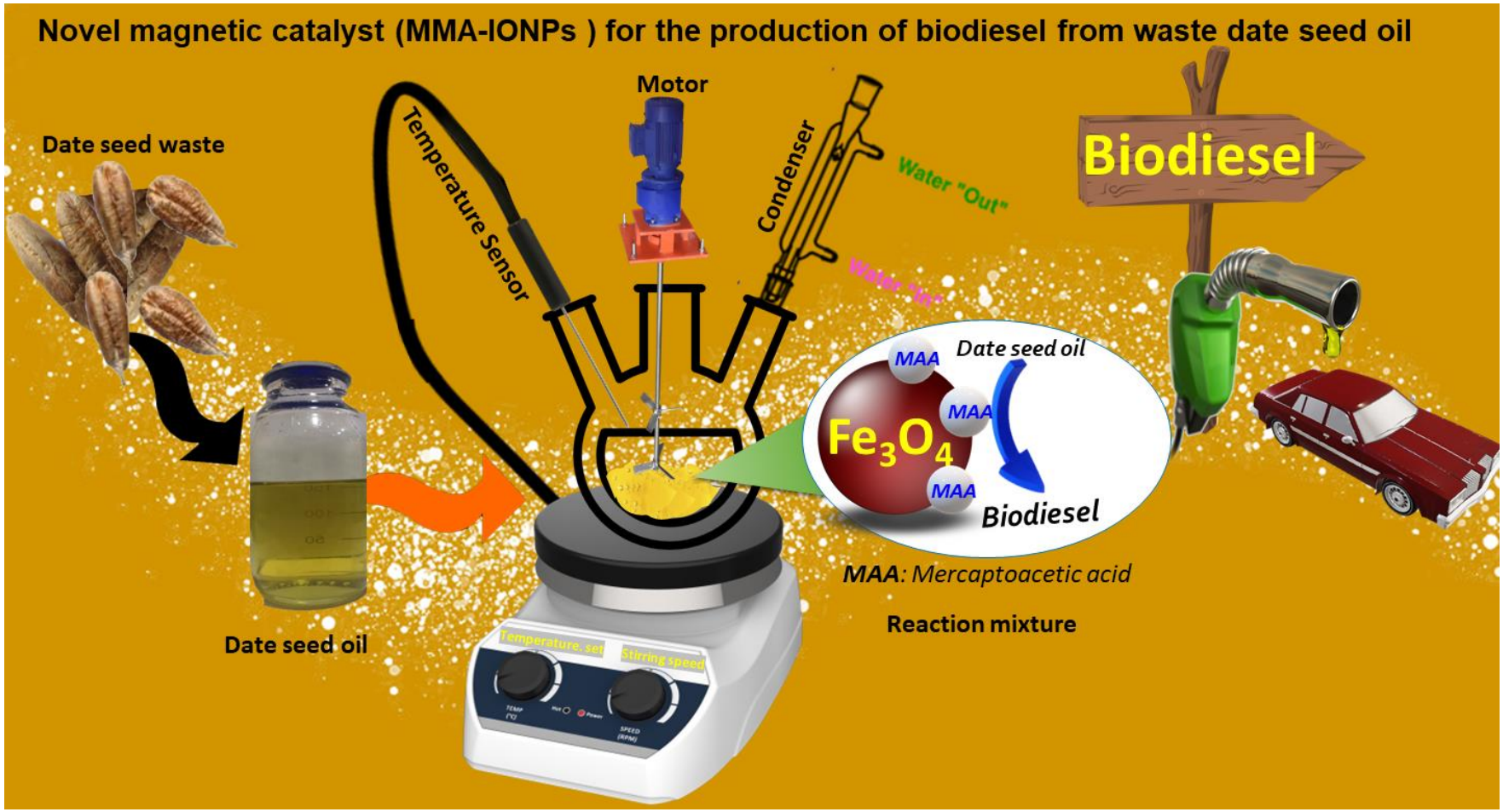

**ABSTRACT:**

The utilisation of waste biomass in biodiesel production as a sustainable energy source can lead to the incorporation of circular bioeconomy principles in the current economic systems. Herein, we synthesised a magnetically recyclable solid acid catalyst for the esterification of waste date seed oil. The catalysts possessed superparamagnetic behaviour and high saturation magnetisation, allowing them to be easily separated from the reaction mixture using an external magnetic filed. The esterification reaction was modelled and optimised by RSM (Design Expert program) and parametric study. The magnetic solid acid catalyst showed high catalytic performance with 91.4 % biodiesel yield with optimum conditions of residence time, catalyst loading and temperature of 47 min, 1.5wt %, and 55 $^{o}$ C, respectively. The solid catalyst was easily recovered by simple magnetic decantation and reused five consecutive times without significant degradation in its catalytic activity. This approach of using waste date seed coupled with cheap magnetic solid acid catalyst has the potential to create more sustainable and cheap catalytic systems for biodiesel production. This will complete the full cycle of waste date seed sustainably and facilitate the development of circular bioeconomy. The LCA results by using CML-IA baseline V3.06 midpoint indicators, for 1000 kg of biodiesel production showed the cumulative abiotic depletion of fossil resources over all the processes as 19037 MJ, global warming potential as 1114 kg $CO_2$ eq, and human health toxicity as 633 kg 1,4-DB eq (kg 1,4 dichlorobenzene eq). The highest damage in all categories was observed during catalyst preparation, and reuse, which was also confirmed in endpoint LCA findings performed using ReCiPe 2016 Endpoint (E) V1.04).

**Keywords:** Biodiesel, Magnetic catalyst, Date seed oil, Life cycle assessment, Parametric study, Circular bioeconomy.

## 1. Introduction

The continuous increase in demand for energy sources pushes humankind to transition from fossil-based linear ecosystems to circular bioeconomy approaches. In this context, circular bioeconomy refers to the sustainable, resource-efficient valorisation of biomass in integrated, multi-output production chains while also using residues and wastes and optimising the value of biomass over time via cascading [1]. Upcycling waste biomass into sustainable fuel will help facilitate economic development in a circular manner providing end uses or other uses in the lifespan of waste lignocellulosic biomass feedstocks, minimising waste and promoting sustainable development [2]. Biodiesel is considered as one of the most accepted alternative transport fuels for diesel engines with comparable physical properties and is being used in diesel engines without or with only minor modification [3]. Biodiesel is fatty acid methyl ester (FAME) produced from vegetable oils such as jatropha oil, sunflower oil, cottonseed oil, soybean oil, palm oil, peanut oil, rapeseed oil and corn oil or other sources like waste cooking oil, animal fats, microalgae and greases [4, 5]. Biodiesel can be produced through the transesterification reaction of triglycerides or the esterification of free fatty acid content in the feed [6]. Contrast to fossil-based diesel, biodiesel is characterised by its high biodegradability along with less toxicity with lower sulfur content and higher flash point than that in diesel fuel [7, 8]. It is worth noting that there are mainly three ways to mitigate climate change and the utilisation of renewable energy is one of the conventional ways [9, 10].

Using non-edible vegetable oil for biodiesel production is a promising solution as it does not compete with food for human consumption [11]. Date seed is a waste part of many date processing industries. Date seeds are a burden as solid waste except a little quantity is used for animal feed such as poultry, camel, sheep and cattle [12]. Massive amounts of date seeds can be

collected from date processing plants and industries by direct or indirect methods [13]. The *Phoenix Dactylifera* (date palm) is the main tree grown in Middle Eastern countries, practically in the Gulf cooperation council countries [14, 15]. In certain countries, the date palm is a major crop, that has covered more than 50% of the overall agriculture area. The main residue of the date palm is the pits, which contain almost 10-15 wt.% of the total residue and is also an inedible part [12]. The amount of oil extracted from the date seed reached 16.5 wt.%, which is further converted into biodiesel through esterification and transesterification processes [12, 14]. Biodiesel derived from waste date seed was recently investigated and shown to possess the fuel properties that meet international standards [16].

Date seed oil cannot be easily converted to biodiesel due to the high content of free fatty acids (FFAs). Thus, the conversion of date seed oil requires more complicated processing. When a basic homogenous catalyst is used for the transesterification of oil feed with FFAs, soaps are formed as a by-product through undesirable saponification reaction leading to a decrease in the produced biodiesel yield [8]. That said, an acidic catalyst can be used to circumvent this issue. A homogenous acidic catalyst such as $H_2SO_4$ can be used with an accurate reduction of acidity [17]. However, this conventional catalyst causes serious contamination problems. The pretreated oil must be completely cleaned from catalytic residual, which are highly corrosive and risky when combusted with fuel [18]. Therefore, several studies have been performed on solid catalysts to convert FFAs into esters by the esterification reaction. Thus, this leads to the formation of methyl ester under acidic condition when methanol is the common alcohol being used herein [19]. Moreover, in the common industrial process, heterogeneous catalysts are a more attractive method for any chemical reactions because they are recyclable, non-corrosive and separable. The use of solid catalysts would also decrease the number of reaction and

92 separation stages required in the transformation of fats and oil to biodiesel, providing for more
93 economical processing and producing high-quality ester product and glycerol [20, 21].

94 Magnetic nanoparticles (MNP) with good properties have found substantial nanomedicine
95 applications, magnetic sealing, separation technology, electronics and catalysis [22, 23]. Among
96 them, magnetite ($Fe_3O_4$) nanoparticles as transition metal oxides are most active and widely
97 applicable. They are easy to synthesise at low cost and are much less toxic than other magnetic
98 nanoparticles [24]. In common applications, magnetite nanoparticles have to be coated with a
99 stabiliser to improve chemical stability, colloidal, and add further functionalisation [25]. The
100 coating is performed using various organic (stabiliser), inorganic and metal materials. Different
101 studies discovered that coating with stabilisers could impact the shape, size, and magnetism of
102 the MNP and other factors such as temperature, concentration, type of anions, ionic strength, and
103 pH or exposure to an external magnetic field [26]. Mercaptoacetic acid is an example of the
104 stabiliser which can be used for coating iron oxide and potentially changing the acidity of the
105 nanoparticles.
106 Furthermore, it works as a catalyst for the esterification reaction to reduce the acid value of oil.
107 The optimum set of operational conditions obtained has been reported [14]: temperature of 70
108 °C, solvent to seed ratio of 4:1 and a time of 7 h, so, the yield of oil extracted at optimum
109 conditions was 16.5 wt.%. Kazemi et al. [27] reported on oil extraction from various date seeds,
110 with the maximum reported was from the Khazravi variety (13.2 wt.%).
111 Therefore, the present study aimed to produce biodiesel using waste date seed oil and iron oxide
112 nanoparticles coated with the mercaptoacetic acid catalyst. Specifically, the objectives of this
113 study were to: (1) synthesise iron oxide nanoparticles coated with the mercaptoacetic acid
114 catalyst from the solvothermal method, which was further used for the esterification reaction of

115 waste date seed oil with methanol; (2) investigate the performance of the catalyst through the
116 parametric study of the practical and mathematical approaches. The effect of various reaction
117 parameters such as catalyst loading, temperature and residence time were studied. Those factors
118 of the reaction conditions were modelled and optimised for the highest catalytic conversion
119 along with better catalyst stability for biodiesel production, and (3) conduct life cycle assessment
120 (LCA) for analysing the environmental feasibility of the biodiesel production process. LCA is a
121 systematic tool that evaluates the environmental impacts of a product through the entire
122 production process, including the primary production process and final disposal after use (ISO:
123 14044) [28].

124 ## 2. Materials and methodology

125 Date seed (*Phoenix Dactylifera L.*) samples were collected from local farmlands. Prior to oil
126 extraction date seeds washed thoroughly and oven-dried. The date seed waste along with its
127 powder form and grinder are shown in Figure S1. Dried date seeds powder is subjected to oil
128 extraction, and extraction was done using AOCS Official Method Am 2-93. Methanol and n-
129 Hexane were purchased from Fisher scientific company (UK). Potassium hydroxide, Ferric
130 chloride hexahydrate and ethanol were purchased from Merck Company (Germany). Ethylene
131 glycol and mercaptoacetic acid were purchased from Alfa Aesar company (Germany). All other
132 chemicals were commercially available and used without further purification.

133 ### 2.1 Characterisation of date seed oil

134 Oil extracted from date seeds is characterised by several techniques to determine its suitability
135 for fuel production. Fatty acid content was determined using GC-MS analysis, and it was done
136 using Shimadzu GC-2010 Plus, fitted with an SP-2560 Supelco capillary column (100 m × 0.250

mm I.D. × 0.2μm film thickness) coupled to GCMS-QP2010 ULTRA MS. Ultra-high purity helium (99.99%) was used as a carrier gas at a constant flow of 1.0 ml/min. The injection, transfer line and ion source temperatures were 250, 240 and 230 ℃, respectively. The ionising energy was 70 eV. Electron multiplier (EM) voltage was obtained from auto-tune. All data were obtained by collecting the full-scan mass spectra within the scan range 35-500 amu. The injected sample volume was 1 μl, with a split ratio of 50:1. The oven temperature program was 50 $^{o}$C (held for 5 minutes) and a heating rate of 4 $^{o}$C. min$^{-1}$ up to 250 $^{o}$C, then held for 5 minutes. The oil compounds were identified by comparing the spectra obtained with mass spectrum libraries (NIST 2011 v.2.3 and Wiley, 9$^{th}$ edition) and further confirmed with Supelco 37 component FAME mixture. FTIR was utilised to identify the functional groups present in the oil sample. Iodine value or iodine number is referred to as a degree of unsaturation of oil sample. The Iodine value was performed as described in the ESI and calculated as in equation 1.

$$Iodine\ Value = \frac{A \times B \times C \times 100 \times 10^{-3}}{D} \quad (1)$$

where, A= equivalent weight of iodine is 127, B = volume of sodium thiosulfate = $V_1 - V_2$, $V_1$= volume (mL) of sodium thiosulfate for a blank test, $V_2$= volume (mL) of sodium thiosulfate for oil sample, C= normality of sodium thiosulfate and D= wt. of oil sample for analysis. The saponification is calculated using Equation 2, then was used for calculating acid value:

$$Saponification\ Value\ (mg\ KOH/g\ of\ oil) = \frac{(B-S) \times N \times M.W}{W} \quad (2)$$

where B is the volume of HCl solution used in the blank run, S is the volume of HCl solution used in the original run, N is the normality of KOH, M.W.= molecular weight of KOH and W= weight of oil sample. The acid value was calculated according to the following equation 3:

$$Acid\ Value\ (mg\ KOH/g\ of\ oil) = \frac{A \times N \times 56.1}{W} \quad (3)$$

Where 56.1 is the molecular weight of KOH (g/mol), N is the normality of KOH (mEq/mL), A is the volume of the KOH (mL) used for titration and W = weight of oil sample (g). The kinematic viscosity of oil samples was measured according to the standard method defined as American Society for Testing and Materials (ASTM) D445-446 by using a Ubbelohde viscometer based on the capillary action.

### 2.2 Catalyst preparation and characterisation

Magnetic $Fe_3O_4$ nanoparticles were synthesised by a solvothermal method, where 2.7g of $FeCl_3 \cdot 6H_2O$ and 5.75g of sodium acetate were dissolved in 50 mL of ethylene glycol and stirred for 1h. The homogeneous yellow mixture solution was then transferred to a Teflon-lined stainless-steel autoclave and heated at 200 °C for 8h. After cooling down to ambient conditions, the black microspheres were separated with an external magnet, washed with ethanol several times, and finally dried in a vacuum oven at 60 °C for 12h. The surface modification of nanoparticles by mercaptoacetic acid was performed using 1g of $Fe_3O_4$ distributed in 80 mL of an ethanolic Mercaptoacetic acid solution (1.74 mmol/L) and constantly stirred for 24 hr. The carboxyl-modified $Fe_3O_4$ (Called as MAA-IONPs) was separated by an external magnetic field and washed with ethanol and water several times. Then the produced catalyst was dried in a vacuum oven at 60 $^{o}$ C for overnight. The catalysts were characterised with different techniques such as Powder X-ray diffraction (XRD), Brunauer–Emmett–Teller (BET) surface area, Scanning electron microscopy (SEM), the thermal gravimetric analysis (TGA), vibrating sample magnetometer (VSM) and Fourier transform infrared spectroscopy (FTIR) with their full description is provided in the ESI.

### 2.3 Esterification reaction and experimental design

Esterification of waste date seed oil using the MMA-IONPs catalyst was carried out in a batch run on a hot plate with a magnetic stirrer at different process conditions. When the reaction was completed, the catalyst was separated by an external magnet and then by filtration to ensure that all the catalyst particles were removed from the biodiesel sample. The biodiesel yield was calculated by using equation 4. Then the acid value was measured and calculated by following the procedure mentioned earlier.

$$Yield(\%) = \frac{weight\ of\ biodiesel}{weight\ of\ oil} \times 100 \quad (4)$$

To investigate the effect of various process parameters on the biodiesel yield, experiments undertaken were selected using Box Behnken Design (CCD) a mode in RSM (Response Surface Methodology), using Design-Expert 9.0 (Stat-Ease, Inc) software. The independent variables selected for consideration were temperature, time and catalyst loading, while the percentage of FFAs conversion (biodiesel yield) was the response variable. Table 1 shows the esterification process conditions and the percentage of FFAs conversions (biodiesel yield) obtained; a total of 14 experiments were required following BBD methodology, including experiments covering all range of independence variables, of which 12 were factorial point and 2 were on the centre point. The range of the independent variables was coded into low (-1) and high (+1) levels, where experiments were repeated twice for reproducibility. Moreover, the experiment was carried out in random order to avoiding any systemic error.

**Table 1:** Experimental plan with varying three process parameters for esterification reaction.

| Run | Time (hr) | T ($^oC$) | S (wt.%) | Biodiesel Yield (%) |
|---|---|---|---|---|
| **1** | 0.5 | 55 | 2.5 | 87.5 |
| **2** | 1.25 | 55 | 3.5 | 82.4 |
| **3** | 2 | 55 | 2.5 | 85.0 |
| **4** | 1.25 | 60 | 2.5 | 74.7 |
| **5** | 2 | 60 | 1.5 | 52.6 |
| **6** | 2 | 65 | 2.5 | 46.1 |
| **7** | 0.5 | 60 | 1.5 | 87.9 |
| **8** | 1.25 | 55 | 1.5 | 91.4 |
| **9** | 1.25 | 65 | 3.5 | 85.7 |
| **10** | 1.25 | 60 | 2.5 | 80.6 |
| **11** | 2 | 60 | 3.5 | 65.4 |
| **12** | 0.5 | 65 | 2.5 | 83.3 |
| **13** | 1.25 | 65 | 1.5 | 80.7 |
| **14** | 0.5 | 60 | 3.5 | 81.1 |

### 2.4 Statistical Analysis

The statistical analysis of the experimental data obtained was performed using a response surface methodology (RSM). The significance of the model was evaluated by the analysis of variance (ANOVA) in which a p-value (probability value) of less than 0.05 was considered significant with 95% confidence, and the coefficient of determination, $R^2$, and lack of fit was assessed to ensure that the predicted model was the most suitable for the experiments undertaken. A parametric study was carried out based on 3D and contour plots obtained using the predicted model, which shows the interactive effect of independent variables on the response factor. The interaction between the response variable and the independent variables was correlated by a model described in equation 5.

$$y = \beta_o + \sum_{i=1}^{k} \beta_{ii} x_{ii} + \sum_{i=1}^{k} \beta_{i=1} {x_i}^2 + \sum i = 1 \sum j = i + 1 \beta_{ii} x_{ii} + \varepsilon \quad (5)$$

Where: y represents the biodiesel, while $\beta_o$, $\beta_{ii}$ and $\beta_{ij}$ are the model coefficients and $x_i$ and $x_{ij}$ are coded factors (independent variables).

## 3. Results and discussion

### 3.1 Characterisation of date seed oil

The oil extracted from date seed was yellow in colour (Figure S2) with a distinct odour. Moreover, it was clear that there were no suspended particles observed. Even after storage for several days of extraction, odour and appearance remained the same, and there was no solid formation. This implies that the oil is highly stable and can be used for different applications without heating and can be extracted and stored for further utilisation in biodiesel production.

The acid value is an intrinsic property of oil which refers to the number of milligrams of potassium hydroxide required to neutralise the free fatty acids present in one gram of oil. As the acid value decreases, the amount of carboxylic acids presents in the oil decreases. The measurement of acid value is crucial before further processing for biodiesel production. Based on this value, all considerations are considered, such as type of catalysts either acidic or basic and whether the oil be directly subjected to transesterification or it should be treated with acidic catalysts to reduce acid value and amount of alcohol. Moreover, it provides information on whether the oil is stable or not, hence measuring its suitability for long storage periods. It is well known that long storage periods can lead to the decomposition of organic matter by oxidation of fatty acids. In the present study, the acid value for date pits was observed to be 20 mg KOH/g.

The date pit oil density was measured using an Anton Paar instrument (DMA 4500M, USA) in accordance with ASTM D-4052 standard method. Density is defined as the amount of oil per

volume. It is an intrinsic property, so it does not depend on the amount of sample but depends on the measuring parameter such as temperature. The density measured of date pits oil was 0.92 $g.cm^{-3}$ at atmospheric conditions. The viscosity was determined following the method specified by ASTM D445. Normally, plant-based oils are highly viscous, thus not appropriate as a direct fuel. So, by alcoholysis for biodiesel production, viscosity is reduced, and this should satisfy international standards. The viscosity of date pits oil was measured to be 23.56 $mm^2.s^{-1}$ which is lower than that of most of the traditional oils currently used for biodiesel synthesis, such as soybean oil 27.45 $mm^2.s^{-1}$ [29], Yucca aloifolia oil 25.86 $mm^2.s^{-1}$ [29] and sunflower oil 29.53 $mm^2.s^{-1}$ [30].

The fatty acid (FA) composition of date pits oil presented in Table 2, shows that date pits oil contains 52.22 % unsaturated fatty acids (UFA) and 47.78 % of saturated fatty acid (SFA). Table 2 shows the FFA profile for some common biodiesel fuel feedstocks, including palm oil, Yucca aloifolia oil and sunflower oil. Table 2 results show that although the amounts of individual fatty acids vary, almost the same acids constitute the fatty acid profiles. The fatty acids derived from different oils used for biodiesel synthesis possess similar fractions and are similar to those currently used in biodiesel production. Thus, by comparing the FA composition of the date pits oil herein along with other feedstocks used for biodiesel synthesis, it can be concluded that date pit oil can be considered a potential feedstock for biodiesel production.

**Table 2:** Fatty acid profile of date pits oil along with fatty acid profiles of other plant-based oils used for biodiesel reported in the literature for comparison to prove the feasibility of date pits oil for biodiesel production.

| | Date Seed Oil | Palm Oil **[31]** | Yucca aloifolia oil **[29]** | Sunflower Oil **[30]** |
|---|---|---|---|---|
| **Lauric (C 12:0)** | 16.36 | 0.26 | - | - |
| **Myristic (C 14:0)** | 13.25 | 2.43 | - | - |
| **Palmitic (C 16:0)** | 15.79 | 46.13 | 8.59 | 7 |
| **Stearic (C 18:0)** | 2.38 | 3.68 | 2.15 | 3.5 |
| **Oleic (C 18:1)** | 45.9 | 37.47 | 13.93 | 33.35 |
| **Linoleic (C 18:2)** | 6.32 | 11.03 | 70.77 | 55.25 |
| **Linolenic (C 18:3)** | - | - | 2.5 | - |

The saponification value for the oil extracted from date pits was 236 mg KOH/g of oil. It has been observed that long-chain fatty acids in fats show a small saponification value as they contain a lower number of carboxylic functional groups as compared with short-chain fatty acids. Thus, the fact that a high value of milligrams of KOH is required for saponification implies the presence of a high quantity of short-chain fatty acid.

The iodine value of oil tends to indicate the degree of unsaturation of oil, which refers to the presence of C=C in the fatty acids. It is one of the major properties to be determined for oil to be transformed into biodiesel as it can also help predict the low-temperature behaviour of oil. The iodine value for date pits oil was determined and found to be 49g of $I_2$/100 g. The date pits oil

contains a higher amount of unsaturated fatty acids, so this can be determined from the iodine value. Rashid et al. [32] reported that Muskmelon oil extracted for biodiesel production has an iodine value of 87.49 g of $I_2$/100 g; thus muskmelon oil has a higher amount of unsaturated fatty acids compared to date pits oil. It has been reported that Moringa Oleifera oil, as a non-edible feedstock and has been used for biodiesel production, showed an iodine value of 70.50 g of $I_2$/100 g [33]. Thus, Moringa Oleifera oil also has more unsaturated fatty acids than date pits oil.

Figure 1a shows the FTIR spectrum of the date seed oil that has been extracted by n-hexane solvent. The absorption band at 584 $cm^{-1}$ represent various inorganic compounds. The absorption band at 721 $cm^{-1}$ is characterised to the aromatic compounds [34], while the absorption bands at 852-1114 $cm^{-1}$ region are represented to the stretching vibration of C-O ester and the $CH_2$ groups. The absorption band at 1160 $cm^{-1}$ is attributed to the C-O stretching alcohols groups. The absorption bands in the region of 1200─1400 $cm^{-1}$ are mostly assigned to the bending vibrations of $CH_2$ and $CH_3$ aliphatic groups like symmetric HCH bending at 1376 $cm^{-1}$ and $CH_2$ scissoring at 1457 $cm^{-1}$. The absorption band at 1744 $cm^{-1}$ is assigned to the C ═ O stretching vibration of carboxylic acids of the ester. The two small absorption bands at 1652 $cm^{-1}$ and 3648 $cm^{-1}$ correspond to the bending and stretching vibration of O-H bonds of the $H_2O$ molecule in the oil [35].

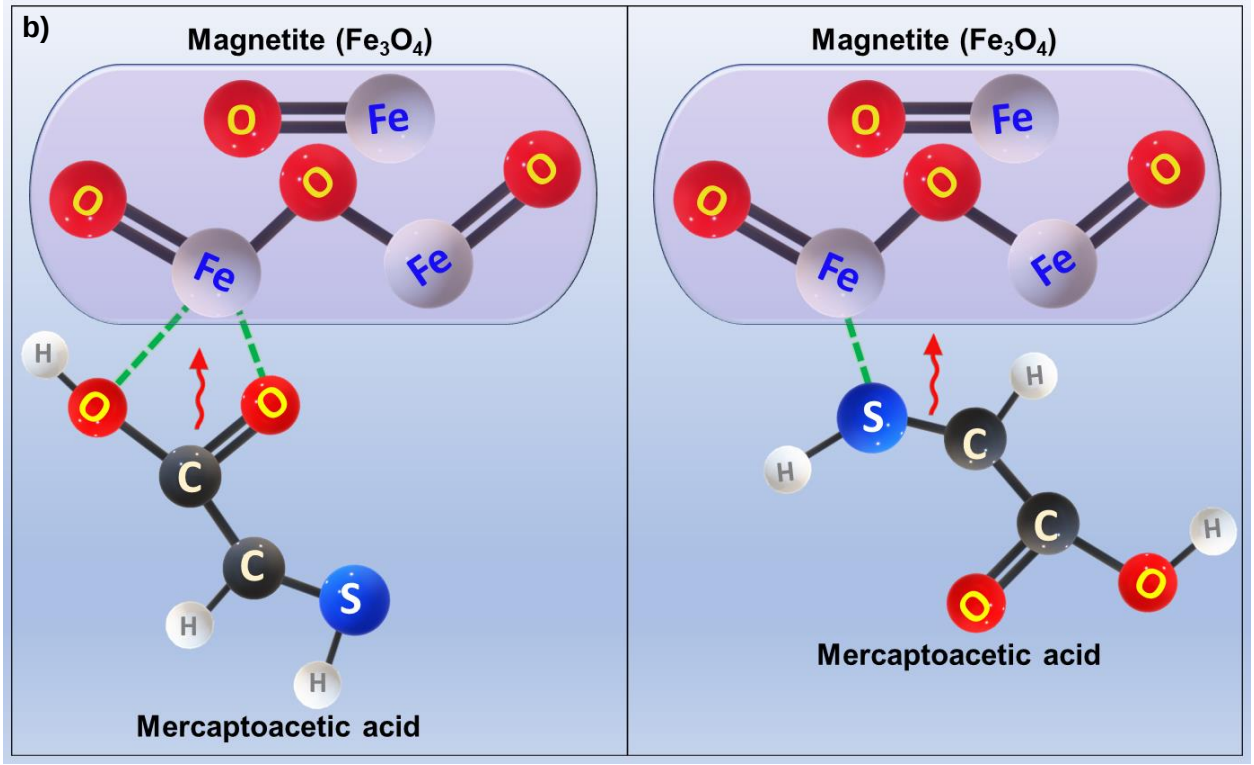


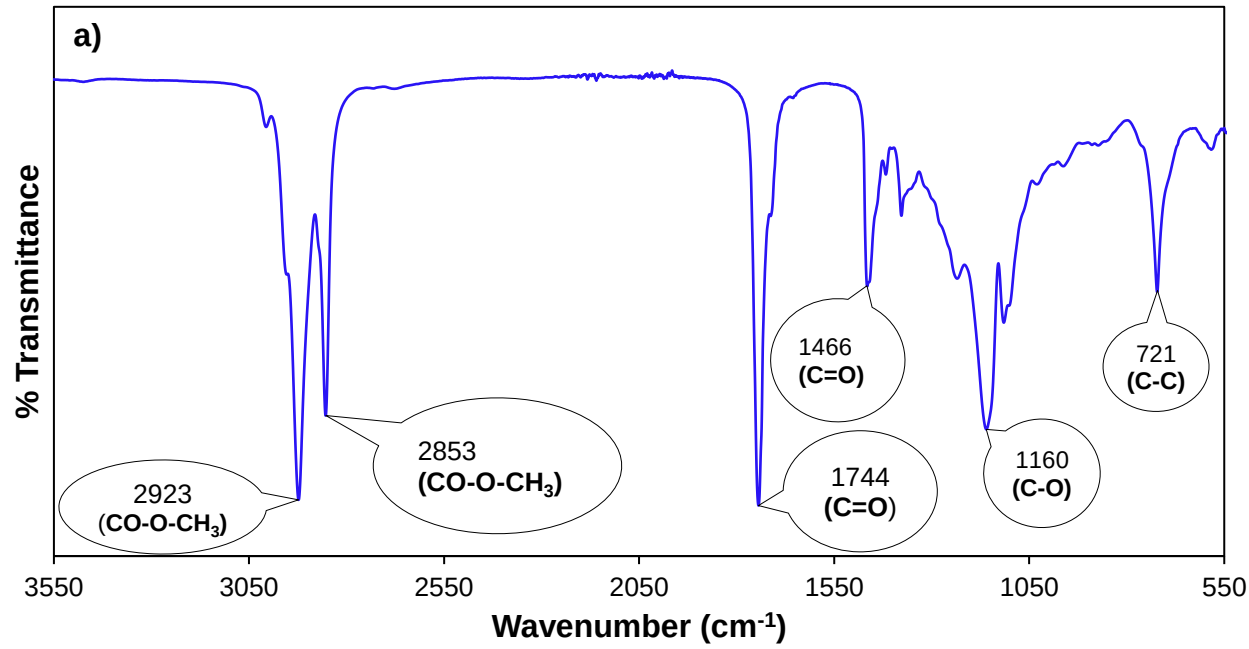


**Figure 1**: shows a) The FTIR spectrum of date seed oil along with b) the schematic representation of the possible attachments of mercaptoacetic acid on iron oxide metal support.

### 3.2 Characterisation of novel magnetic catalyst

Herein a magnetic solid acid catalyst was synthesised with the advantages of easy separation and reusability compared to homogenous catalysts. It consists of mercaptoacetic acid supported on iron oxide nanoparticles ($Fe_3O_4$) as an acidic catalyst. The schematic representation for the attachment of mercaptoacetic acid on iron oxide nanoparticles (IONPs) is shown in Figure 1b, where the iron metal is bonded to either the carboxylic group (-COOH) or the mercaptans group (S-H). The XRD analysis of IONPs and the modified mercaptoacetic acid-iron oxide nanoparticles by (MMA-IONPs) are shown in Figure 2a. The diffraction lines of IONPs are attributed to the XRD for iron oxide nanoparticles at 2θ of 18.2, 30.1, 35.4, 43, 53.4, 56.9 and 62.6$^o$ (JCPDS card no. 39-1346), so the preparation of nanoparticles was achieved with a calculated particle size of 27.7 nm [36]. The comparison between the synthesised catalyst herein and the literature is shown in Table S1, where other catalyst prepared with the same solvothermal method showed particle sizes of 45-80 nm [37]. The MMA-IONPs also have the same diffraction lines as IONPs; thus, iron oxide nanoparticles' coating material did not affect the crystalline of the IONPs.The surface morphology and elemental composition of synthesised catalysts were analysed by SEM and EDS, as shown in Figure 2b. The IONPs catalyst's micrographs showed spherical particles; also, the introduction of MMA-IONPs displayed a similar shape with a difference in the distribution of nanoparticles on the surface. The corresponding EDS result showed that the wt.% of C element for nanoparticles uncoated and nanoparticles coated presented 13.6 and 26.2 wt.%, respectively. While for the iron element, the values were 59.7 and 43.6 wt.%, respectively. These results confirm the nanoparticles' coating by the organic material, because the percentages of carbon, present in MMA-IONPs, increased approximately by 12.6 wt.% after coating.

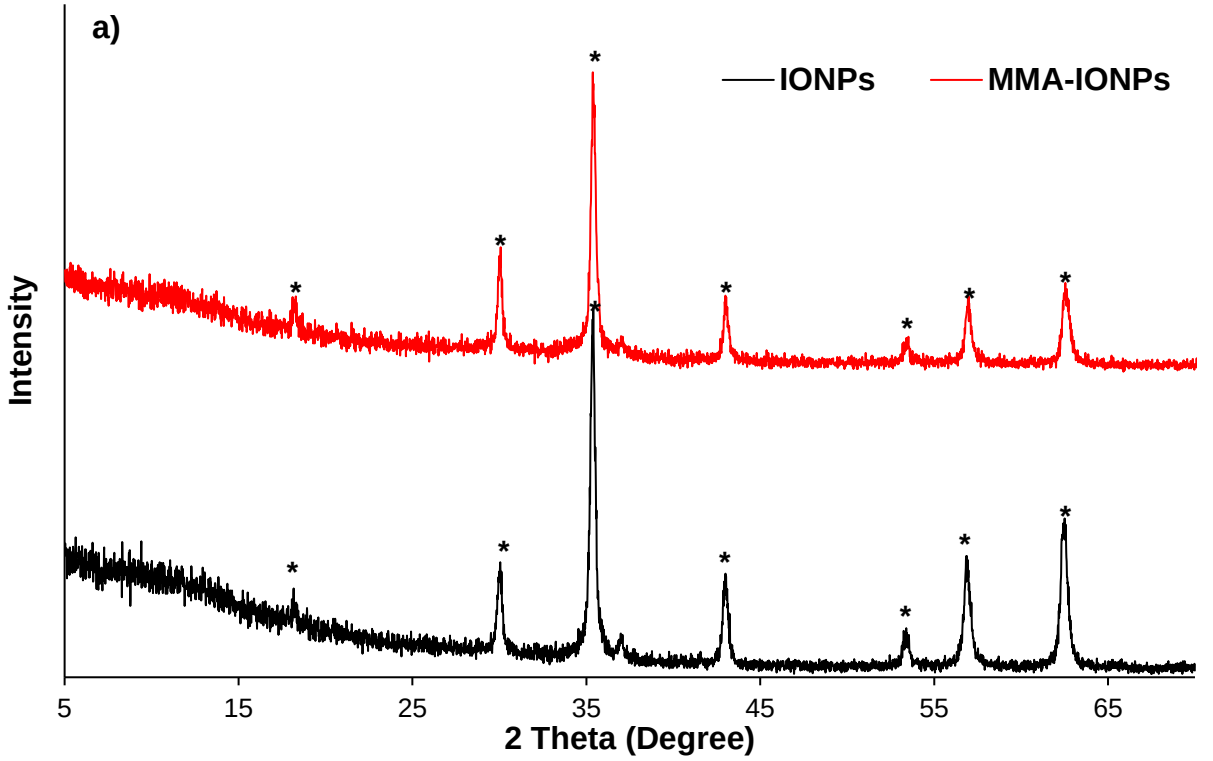


313

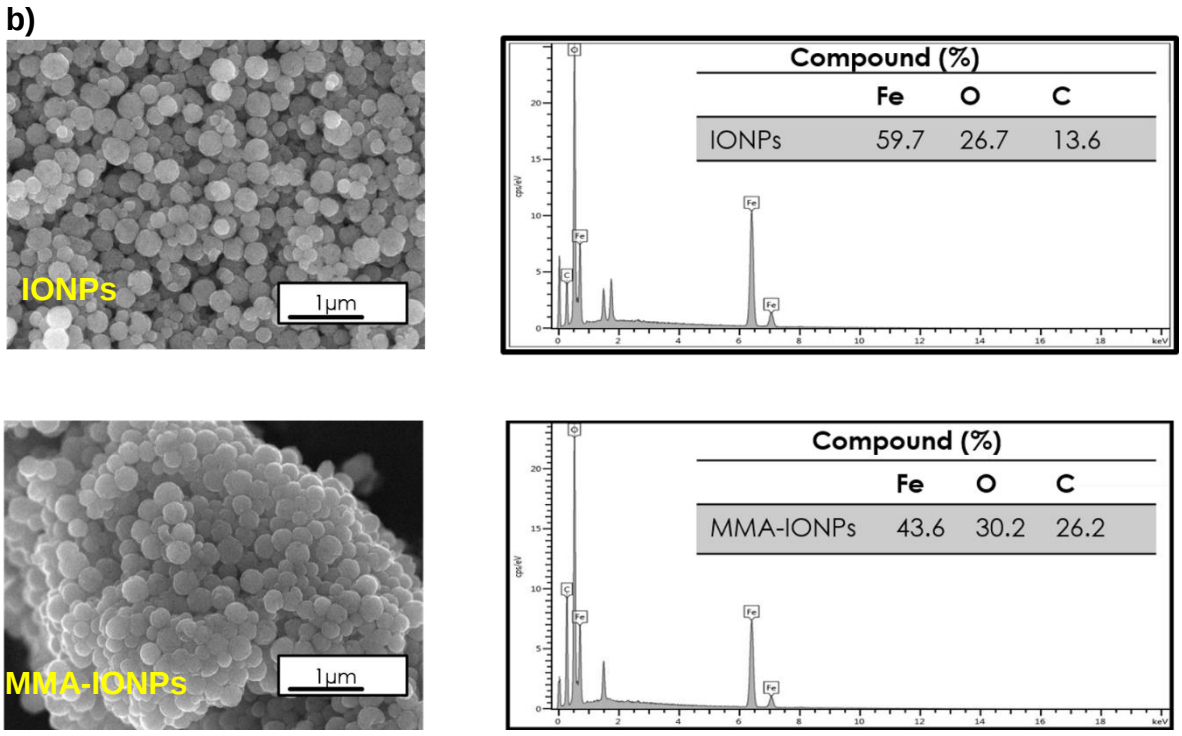


314

315 **Figure 2:** shows a) X-ray diffraction of IONPs and MMA-IONPs along with b) SEM/ EDS of

316 IONPs and MMA-IONPs catalysts.

The behaviour of the iron nanoparticles in water or toluene can be observed in Figure 3. The pure magnetic nanoparticles remain suspended in the aqueous medium due to the oxide material's hydrophilic surface, as shown in Figure 3a. Figure 3b demonstrates the suspension of iron nanoparticles coated by mercaptoacetic acid in between water and toluene. Obviously, coating with organic material makes them hydrophobic and apart from water into between the two-phases. This behaviour revealed that the novel catalyst was an amphiphilic compound which can dissolve in two phases.

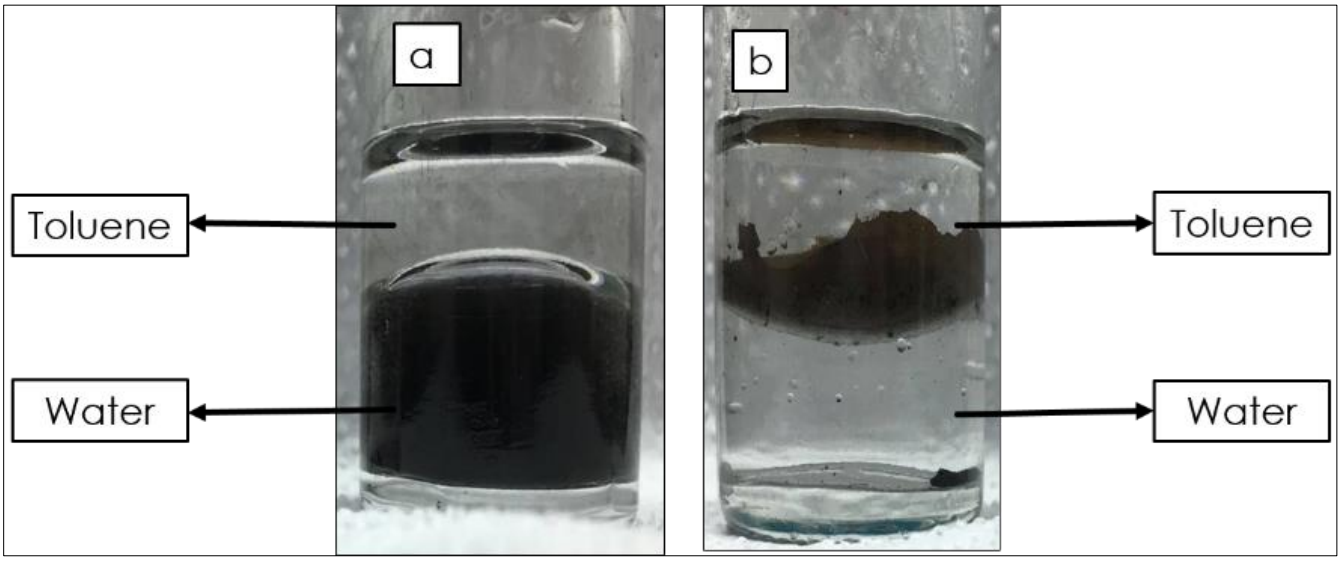


**Figure 3:** the behaviour of pure iron nanoparticles (IONPs) and coating nanoparticles (MMA-IONPs) in the water-toluene system.

The FTIR spectra of Figure S3 compares the pure iron oxide nanoparticles (IONPs) and the modified mercaptoacetic acid- iron oxide nanoparticles (MMA-IONPs). The nanoparticles of iron oxide (IONPs) showed absorption bands in the region of 571 and 620 $cm^{-1}$, attributed to the Fe-O group. The band at 1724 $cm^{-1}$is related to the carbonyl group's stretching of the carboxylic anhydride and generates an overlapping of C=O band [38]. The bands at 1630 and 3400 $cm^{-1}$ are

assigned to the OH group's vibration coated on the surface of iron oxide [39]. The symmetric and asymmetric stretching of CH groups in the MMA-IONPs are observed at 2856 and 2925 $cm^{-1}$, respectively [40]. Thermogravimetric analysis was done to investigate the modified catalyst's thermal degradation by mercaptoacetic acid- iron oxide nanoparticles (Figure 4a). The thermogravimetric curve of pure nanoparticles showed weight loss of approximately 1 wt.%, where the first mass loss step occurred at relatively 100 °C, which is related to the water adsorbed on the surface of the magnetite nanoparticles. Unlike the pure magnetite nanoparticles, the MMA-IONPs showed three weight loss stages with a higher weight loss of 2.25 wt.% compared to the pure magnetite nanoparticles catalyst. The first, second and third weight losses were observed at temperature ranges of 130-140, 280-300 and 380-390 °C, respectively. Those three weight loss stages may be attributed to the decomposition of the mercaptoacetic acid within the MMA-IONPs modified catalyst.

Moreover, the TGA graph showed that the MMA-IONPs catalyst is not stable at 136 °C. The magnetic behaviour of iron oxide nanoparticles and the modified nanoparticles coated with the organic materials can also be observed from the magnetisation measurements at room temperature (Figure 4b). Both samples possess typical superparamagnetic behaviour. The uncoated particles' saturation magnetisation was 85.5 emu/g, and the corresponding value for the modified nanoparticles coated with organic material was 75.5 emu/g. This implies a good distribution of the coated modified nanoparticles onto the iron nanoparticles. The magnetisation of the modified coated nanoparticles was very high as the thickness of the coating material was small due to the short-chain hydrocarbons distributed around the nanoparticles. The nitrogen adsorption-desorption isotherms of $Fe_3O_4$ and MMA-$Fe_3O_4$ catalysts are shown in Figure 4c. The $S_{BET}$ and pore volume of $Fe_3O_4$ were 88.5 $m^2.g^{-1}$ and 0.11 $cm^3.g^{-1}$, respectively. While in MMA-

$Fe_3O_4$ catalyst those values dramatically decreased to 13.4 $m^2.g^{-1}$ and 0.08 $cm^3.g^{-1}$, respectively which may be due to the attachment of mercaptoacetic acid on the $Fe_3O_4$ support, thus offering another evidence of the successful coating of organic material. The small porous volume of MMA-IONPs is due to the covering of the organic material of the mercaptoacetic acid into the pores of the IONPs support.

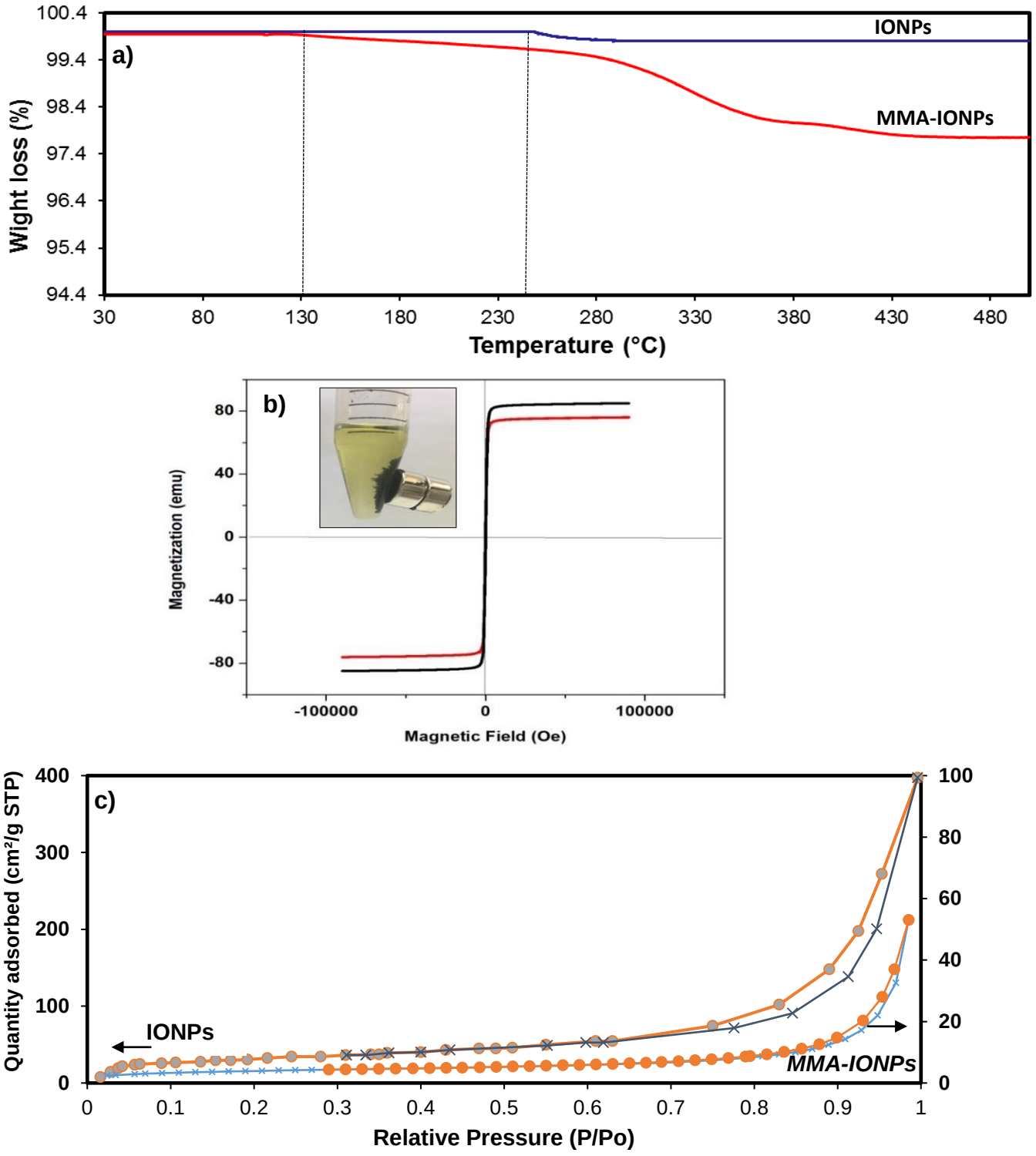


376

377

**Figure 4**: shows a) TGA analysis for IONPs and MMA-IONPs, b) vibrating-sample magnetometer of IONPs and MMA-IONPs along with c) The $N_2$ adsorption-desorption of IONPs and MMA-IONPs catalyst.

### 3.3 Esterification reaction using the synthesised catalyst

It has been reported that methanol is the most suitable alcohol for the esterification process [41]. Esterification was studied herein by varying three parameters, including temperature, residence time and catalyst load within the process to measure their impact on the biodiesel yield (conversion of FFA). The RSM based experimental plan, along with biodiesel yield (which occurs due to FFA and triglycerides conversion) obtained for each experimental test, are reported in Table 1. Moreover, a blank test between methanol and oil was performed and observed to have negligible (5.3% ±1.0) formation of methyl ester formation. It was noticed that biodiesel yield based on the defined experimental conditions varied from 46 to 91 wt.%. The main aim of using RSM was to study the combined effects of process parameters on FFA conversion (biodiesel yield) along with the statistical analysis. Meanwhile, the results related to statistical analysis of extraction process and parametric analysis of FFA conversion based on RSM, are discussed in detail in the following sections.

### 3.4 Determination of statistical model

Based on the regression analysis, a reduced quadratic model predicted in terms of coded factors for the response factor (biodiesel yield) was found, as shown in equation 6:

$$Biodiesel\ Yield\ (\%) = 0.00122 + 0.0026A + 0.0002B - 0.0003C + 0.0023AB - 0.0012AC + 0.0022A^2 + 0.0024A^2B \quad (6)$$

A p-value of less than 0.05 shows the significance of the model at a 95% confidence level; however, lack of fit should be non-significant for the appropriate model [42]. Lack of fit compares residual error and pure error which should be insignificant for a significant model.

However, as shown in Table 3, the p-value for the selected model was less than 0.05, implying that it is significant, with a 95% confidence level.

**Table 3:** ANOVA results given by RSM based on which the significance of the predicted model is checked along with each parameter.

| Source | Sum of | df | Mean Square | F-Value | P-value | |
|---|---|---|---|---|---|---|
| Model | 0.00 | 7 | 0.00 | 23.7 | 0.0006 | significant |
| **A-t** | 0.00 | 1 | 0.00 | 70.2 | 0.0002 | |
| **B-T** | $2x10^{-7}$ | 1 | $2 x10^{-7}$ | 0.4 | 0.5927 | |
| **C-S** | $6x10^{-7}$ | 1 | $7 x10^{-7}$ | 0.9 | 0.3898 | |
| **AB** | 0.00 | 1 | 0.00 | 28.9 | 0.0017 | |
| **AC** | $5 x10^{-6}$ | 1 | $5 x10^{-6}$ | 7.3 | 0.0359 | |
| **$A^2$** | 0.00 | 1 | 0.00 | 22.0 | 0.0034 | |
| **$A^2B$** | 0.00 | 1 | 0.00 | 14.9 | 0.0083 | |
| Residual | $4x10^{-6}$ | 6 | $7 x10^{-7}$ | | | |
| **Lack of Fit** | $4. x10^{-6}$ | 5 | 8.134E-07 | 1.7 | 0.5230 | not significant |
| **Pure Error** | $5 x10^{-7}$ | 1 | 4.801E-07 | | | |

Analysis of variance (ANOVA) for the experimental data with the predicted model (Table 3). The predicted model was highly significant for this experimental data due to the high F-value of 23.7 and p-value of less than 0.05. A significance can be observed for term A (time of contact) and interactions of variables AB and AC and quadratic form of some variable such as $A^2$ and quadratic interaction form such as $A^2B$. However, factor B (temperature) and C (loading) have less effect as a function of FFA conversion. The coefficient of variation is the ratio of the standard deviation and the mean of data. It is about 6.5, which describes the significant degree of precision with a high reliability of the suggested model's experimental data.

Moreover, the coefficient of determination ($R^2$) was close to unity, as shown in Table S2. The predicted $R^2$ of 0.8522 is reasonably agreed with the adjusted $R^{2,}$ where the difference is less

than 20 %. Besides, adequate precision measures the signal to noise ratio where the ratio greater than 4 is desirable [43]. The suggested model has a ratio of 16.7, which indicates an adequate signal. Table S2 supports the suggestion that the experimental data fit well with the model and provides an estimation of the system's response factors in the range considered.

### 3.5 Effect of operating variables on biodiesel yield

To study the effect of process parameters on biodiesel yield, 3D plots were used which provide the combined effect of two process variables. The combined effect of time of contact and process temperature on the response factor, while catalyst loading was kept constant, as shown in Figure 5, was investigated using a 3D plot and 2D contour plot. For both the 3D and 2D contour plots, the time varied between 30 min to 2 hr. The operating temperature ranged from 55 to 65 °C, while catalyst loading was kept constant at 2.5 wt.% of the pretreated oil weight. The biodiesel yield increased with decreasing the contact time. However, it is important to note that the amount of acid value of date seed oil is not affected directly by the reaction temperature. Thus, when the reaction reached a high temperature at the low contact time, the biodiesel yield was maximised. As the reaction temperature increased near the alcohol boiling point, the reaction mixture tends to be in one phase (methanol/oil), and the conversion was maximised. The curvilinear nature of 3D and 2D contour plots depicts the significance of an interactive effect on biodiesel yield as the maximum value of the response factor was found at a lower time of contact.

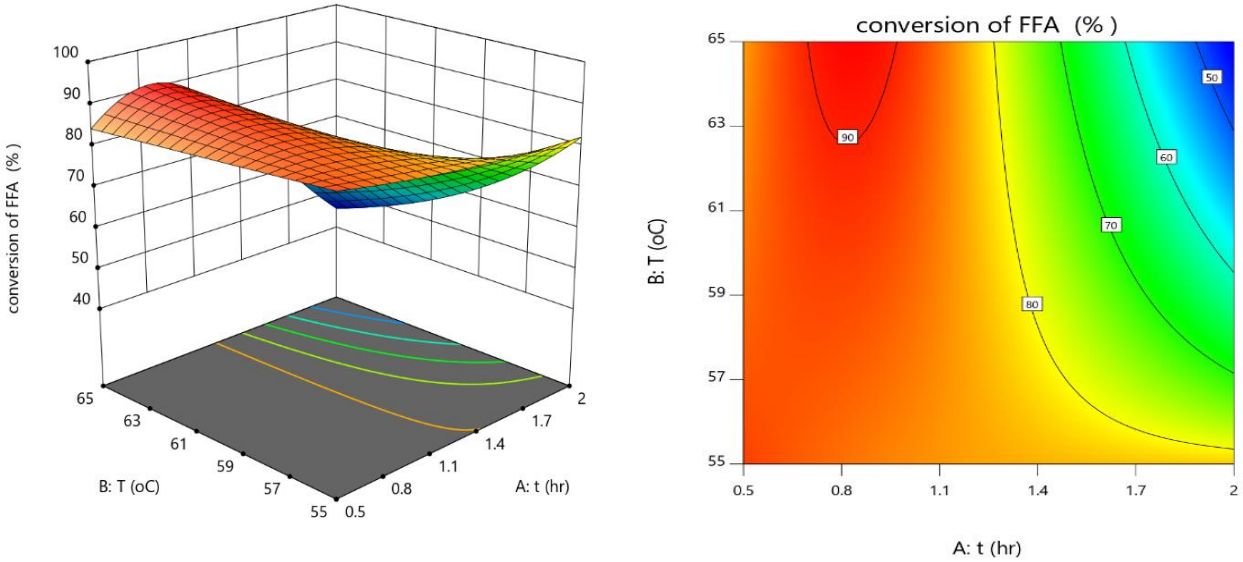


**Figure 5:** 3D and contour 2D plots for analysing the combined effect of contact time and process temperature on the FFA conversion (*biodiesel yield*) of date seed oil.

The interactive effect of time of contact (0.5-2 hr.) and catalyst loading (1.5-3.5 wt.% of oil weight) on the value of biodiesel yield when the temperature was kept constant (65 °C) is shown in Figure 6 by 3D and 2D contour plots. It is obvious that as the time of contact increases, the biodiesel yield decreases. On the one hand, at low catalyst loadings along with low contact time, this scenario can maximise the biodiesel yield. In contrast, the high catalyst loading provided high biodiesel yield of approximately 85 wt.%, when the time contact was low. Thus, the acid value was reduced to 2 mg KOH/g of oil at a low catalyst loading with low reactions occurring.

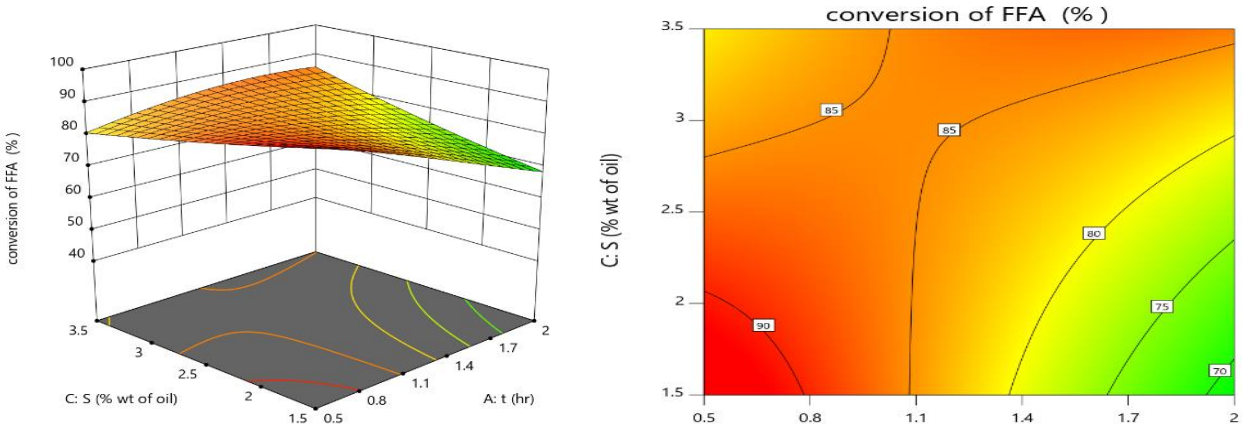


**Figure 6**: 3D and contour 2D plots for analysing the combined effect of contact time and catalyst loading on the FFA conversion (biodiesel yield) of date seed oil.

The optimisation condition that can maximise the biodiesel yield of date seed oil, minimise the operating temperature and minimising the catalyst loading are shown in Figure 7. This operating condition was used to investigate the activity of the catalyst. The optimum time, temperature and catalyst loading was 0.7 hr., 55 °C and 1.5 wt.% of pretreated oil, while the biodiesel yield was 90%. The optimum conditions for the esterification reaction using the MMA-IONPs had lower catalyst loading, contact time and operating temperature than other catalysts. Moreover, the percentage conversions of FFA were high in both MMA-IONPs and Al-SA catalysts with values of 90, 92.6 %, respectively.

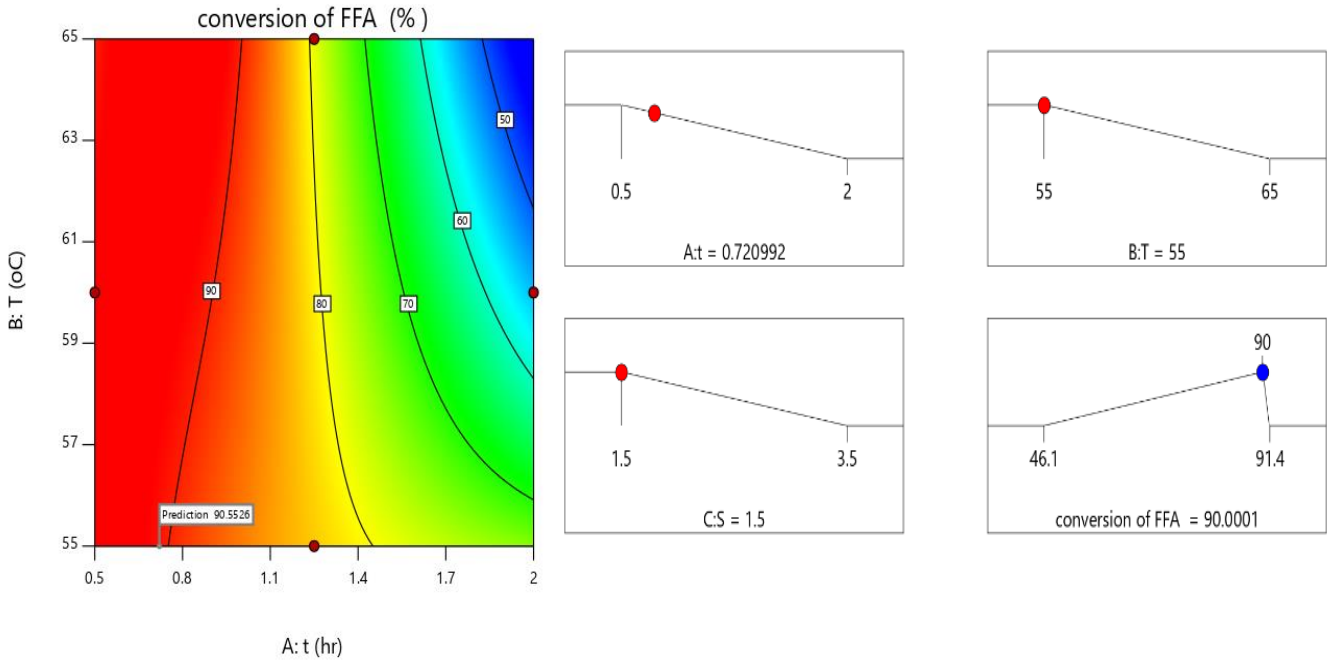


**Figure 7:** optimisation condition of all parameter for high FFA conversion.

### 3.6 Catalyst reusability and activity

Reusability of catalysts is a crucial characteristic when considering upscaling the process on the industrial scale. MMA-IONPs catalysts' reusability was determined based on the optimal set of conditions such as temperature 55 °C, time 42 min., catalysts loading 1.5 wt.% and methanol to oil ratio 15:1. Esterification of free fatty acids was performed repeatedly for five times, as shown in Figure 8. After each run, the catalyst was recovered, rinsed with ethanol to remove the remaining organic components followed by water washing and then to dry in a vacuum oven at 60 °C for 12 hrs. The catalyst's reusability revealed that the MMA-IONPs catalyst is to maintain its catalytic activity for five times without any significant decrease in the biodiesel yield. Based on the FTIR spectrum analysis, the catalyst was active with the origin catalyst's same absorption bands, as shown in Figure S4.

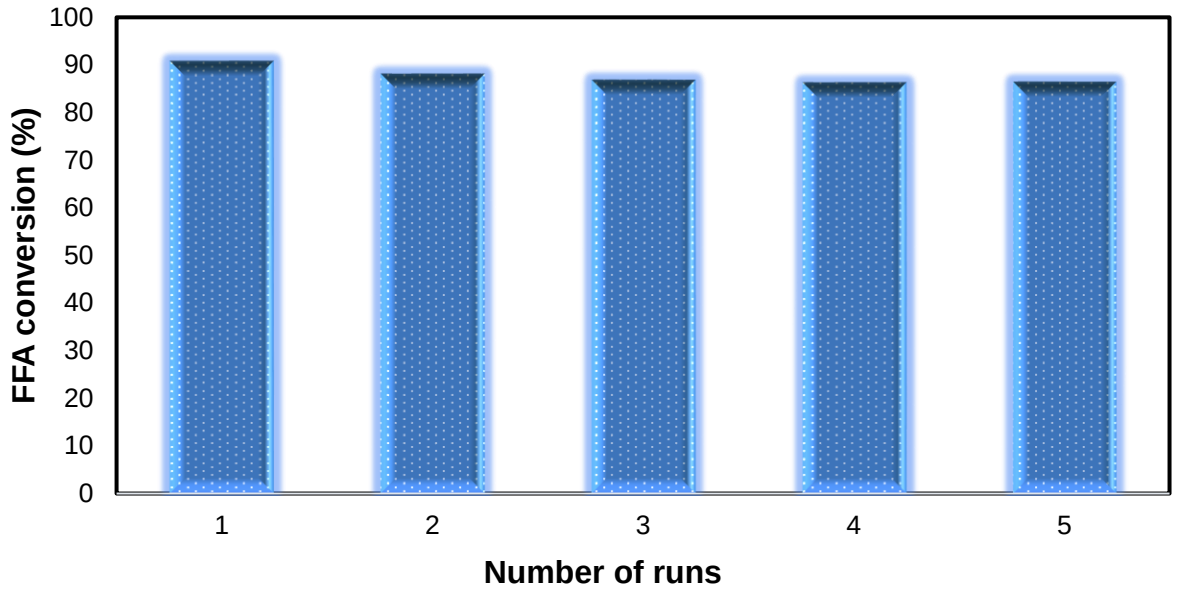


**Figure 8:** Reusability of synthesised catalyst for FFA conversion (*biodiesel yield*) on an optimised set of conditions for esterification.

### 3.7 Life cycle assessment

#### 3.7.1 Goal and scope

The goal of using LCA in the current study was to evaluate environmental and human health impacts of biodiesel product from date seed oil, considering the guidelines provided by ISO: 14040 and ISO: 14044 [28, 44]. The functional unit in this study is 1000 kg of biodiesel produced using date seeds as raw material. The LCA system boundary consisted of raw material transportation, raw material preparation for date seeds to date seed oil, catalyst preparation and reuse, and esterification for biodiesel preparation (Figure 9). The waste products from the system included gaseous emissions, wastewater and solid cake for which the impacts were not considered.

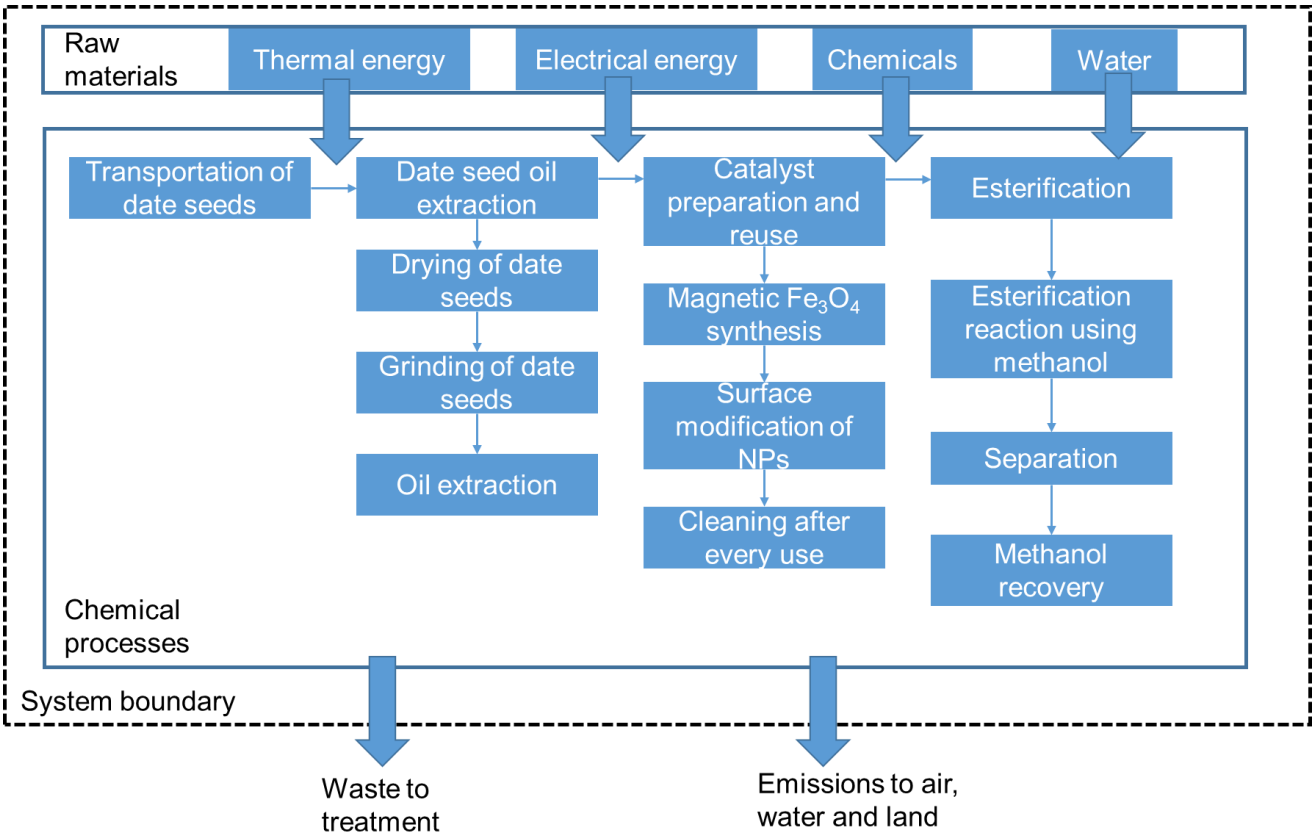


478

479 **Figure 9:** System boundary for life cycle analysis of biodiesel production.

480 **3.7.2 Inventory analysis**

481 This LCA has a cradle-to-gate attributional approach and did not include any infrastructure
482 processes related to lab equipment production. The production of date seeds was not considered
483 part of the system boundary, as it was a waste source. The raw material transportation for 200
484 km was considered in the present study from farms to the oil extraction centre for date seeds
485 (Table 4). Prior to oil preparation, date seeds were dried, and the energy requirement was
486 adapted from operating parameters of the instrument. However, the present study applied soxhlet
487 extraction, as date seed oil was used for conversion in the laboratory. That said, large-scale
488 processing of date seed oil to produce biodiesel would benefit from an application of commercial
489 processes including drying, cooking of seeds, conversion of date seeds to flakes and expeller,

with energy requirements from instrument operating conditions and Fridrihsone et al. [45]. However, only 10% efficiency was considered from this process, as generally the extraction without solvents is less efficient. No weight loss was considered during the cooking of seeds.

In addition to biodiesel production using date seed oil, catalyst preparation and reuse were also considered part of the LCA subsystem. It was observed that the best yield of date seed oil was at 1.5 wt% of catalyst for date seed oil (Section 3.5) Accordingly, producing 1000 kg of biodiesel requires 3 kg of a catalyst by reusing the same catalyst four times. The precursor mass requirement was referred from the catalyst preparation process (Section 2.2). It was assumed that the surface coating of NPs does not lead to a change in molecular weight. Moreover, the wastewater and ethanol mixture were used to clean the catalyst after use, for 1 kg of catalyst cleaned 1 l of water and ethanol mixture to be utilised. After considering losses of cleaning mixture (10%), this process led to the production of wastewater [46]. Moreover, electrical energy requirements were considered from Marimón-Bolívar and González [47]. Additionally, the location of the catalyst preparation unit was considered to be in the vicinity of the biodiesel production plant, and thus the transportation of catalyst was not considered as part of LCA.

The feedstocks for esterification included methanol, catalyst and date seed oil. The findings from the experiments showed the use of methanol: oil as 15:1 and 1.5 wt% of oil as a catalyst (section 3.6). The required energy for carrying out esterification was referred from Dufour and Iribarren [48]. The amount of catalyst at the end of the reaction was assumed to be constant as no catalyst consumption was assumed in the reaction. Moreover, the present study showed an efficiency of 90% for oil to biodiesel conversion. Therefore, 1111.11 kg of date seed oil and 15 kg of catalyst (3 kg used four times) and 74.07 kg of methanol lead to biodiesel production (1000.00 kg). The methanol losses were considered due to evaporation.

513 Moreover, there was the energy required for separation, filtration and centrifugation, which was
514 considered to be 2% of the esterification process. The material losses due to the use of filters
515 were neglected in the LCA process. Recovery of methanol and corresponding energy
516 requirements were calculated using Eq. 7 and 8, according to Barjoveanu et al. [49].

517 $Qa = m. Cp. \Delta T$ (7)

518 $Qm = hc. A. \Delta T$ (8)

519 *where, Qa is the energy required for heating (kWh), Qm is the energy for maintaining required*
520 *temperature (kWh), m is the mass of heated fluid (kg), Cp is the specific heat, (kW/kg K), hc is*
521 *the global heat transfer coefficient, (W/m$^2$ K), A is the heated surface area, ΔT is the temperature*
522 *difference (degrees).*

523 **Table 4:** Inventory analysis for LCA of production of 1000 kg of biodiesel.

| Inventory item | Unit | Input | Output | Reference |
|---|---|---|---|---|
| **Raw material transportation** | | | | |
| **Diesel** | kg | | | |
| **[a] Transportation** | tkm | | 2777.78 | Based on calculation (t*km) |
| **Oil extraction** | | | | |
| **[b] Electricity for drying seeds** | kwh | 30.72 | | Instrument [50] (Drying oven) |
| **Electricity for cooking seeds** | kwh | 138.75 | | Instrument [51] |
| **Electricity for seed flaker** | kwh | 77.76 | | Instrument [52] |
| **Electricity for oil extraction** | kwh | 503.64 | | [45] |
| **Date seeds** | kg | 13888.88 | | Oil extraction process (Section 2.1) |
| **Dried date seeds** | kg | | 11111.1 | |
| **Solid cake** | kg | | 8666.66 | |
| **Loss** | kg | | 222.22 | |
| **Date seed oil** | kg | | 1111.11 | |
| **Catalyst preparation and reuse** | | | | |
| **$FeCl_3.6H_2O$** | kg | 10.51 | | Catalyst preparation process (Section 2.2) |
| **Sodium acetate** | kg | 22.38 | | |

| | | | | |
|---|---|---|---|---|
| **Ethylene glycol** | l | 194.63 | | |
| **Mercaptoacetic acid** | l | 37.5 | | |
| **Ethanol (50% v/v)** | kg | 0.001 | | |
| **Electricity for synthesis** | kwh | 138.00 | | Marimón-Bolívar and González (2018) [47] |
| **[c] Thermal energy for synthesis** | MJ | 138.00 | | |
| **Catalyst** | kg | | 3.00 | |
| **[d] Catalyst reuse for four runs** | kg | | 12.00 | Catalyst reuse process (Section 3.6) |
| **Water** | l | 6 | | |
| **Ethanol** | l | 6 | | |
| **Wastewater** | l | | 10.80 | Chung et al. (2019) [53] |
| **Electricity for drying** | kwh | 2.48 | | Instrument operation [50] |
| **Esterification** | | | | |
| **Date seed oil** | kg | 1111.11 | | Esterification reactions (Section 3.5) |
| **Methanol** | kg | 74.07 | | |
| **Thermal energy for esterification** | MJ | 222.30 | | Dufour and Iribarren (2012) [48] |
| **Electricity for esterification** | kWh | 31.43 | | |
| **[e] Biodiesel** | kg | | 1000.00 | |
| **Electricity for separation** | kWh | 0.06 | | 2% of esterification energy |
| **Thermal energy for separation** | MJ | 4.44 | | |
| **Methanol recovered (95%)** | kg | | 70.37 | |
| **Electricity for methanol recovery** | kwh | 91.3 | | Eq. 7 and 8 |

[a] *Transportation: Lorry transport, Euro 0, 1, 2, 3, 4 mix, 22 t total weight, 17,3 t max payload RER*

[b] *Electricity, production mix PK (WFLDB 3.1)/PK U*

[c] *Calorific value of natural gas: 42 MJ/kg*

[d] *Total consecutive use of catalyst was considered for five runs (reuse for four runs).*

[e] *Biodiesel calorific value: 41.39 MJ/kg*

### 3.7.3 Midpoint indicator assessment

In this study, midpoint indicator assessment was conducted using CML-IA baseline V3.06 to better understand and compare the impact categories. LCA of the biodiesel production process was conducted based on four stages in the inventory analysis: raw material transportation, oil extraction, catalyst preparation and reuse, and esterification to produce 1000 kg of biodiesel (1

functional unit). The waste treatment processes and emissions to air, water and land were not considered as part of LCA, as shown in system boundary in Figure 9.

Table 5 shows the results of the midpoint indicator assessment. Esterification showed the least environmental impacts followed by raw material transportation. This is due to the distance consideration of 200 km in the present study.

**Table 5.** Environmental impacts due to biodiesel production process (1000 kg) computed using CML-IA baseline V3.06.

| Impact category | Unit | Raw material transportation | Oil extraction | Catalyst preparation and [a] reuse | Esterification |
|---|---|---|---|---|---|
| **Abiotic depletion** | kg Sb eq | 0.00 | 0.00 | 0.02 | 0.00 |
| **Abiotic depletion (fossil fuels)** | MJ | 1282.11 | 2439.34 | 14503.26 | 812.09 |
| **Global warming (GWP100a)** | kg $CO_2$ eq | 91.53 | 247.74 | 726.80 | 48.18 |
| **Ozone layer depletion (ODP)** | kg CFC-11 eq | 0.00 | 0.00 | 0.00 | 0.00 |
| **Human toxicity** | kg 1,4-DB eq | 2.86 | 119.44 | 489.70 | 20.96 |
| **Fresh water aquatic ecotox.** | kg 1,4-DB eq | 0.05 | 161.06 | 324.89 | 26.69 |
| **Marine aquatic ecotoxicity** | kg 1,4-DB eq | 1222.86 | 472924.54 | 834714.31 | 78797.35 |
| **Terrestrial ecotoxicity** | kg 1,4-DB eq | 0.00 | 0.35 | 0.90 | 0.06 |
| **Photochemical oxidation** | kg $C_2H_4$ eq | 0.03 | 0.05 | 0.38 | 0.01 |
| **Acidification** | kg $SO_2$ eq | 0.43 | 1.37 | 3.07 | 0.26 |
| **Eutrophication** | kg $PO_4^{---}$ eq | 0.10 | 1.04 | 1.12 | 0.17 |

*[[a] Catalyst reuse was considered for four runs]*

For oil extraction on a commercial scale, depletion of fossil fuels (2439.34 MJ) and global warming potential (247.74 kg $CO_2$ eq) were observed. The catalyst preparation and reuse for four cycles showed abiotic depletion of fossil fuels as 14503.26 MJ and global warming potential as 726.8 kg $CO_2$ eq. This is due to high electricity input for catalyst preparation. The final stage

evaluated for LCA was esterification to produce biodiesel. This stage's inputs were date seed oil, catalyst, methanol, and electricity, leading to depletion of fossil fuels as 812.09 MJ.

Relative results were generated from the simulation for which indicator results maximum is set 100%. Figure 10 shows that catalyst preparation and reuse are above all other processes in terms of impact categories. This is due to energy use in thermal and electricity forms, leading to emissions related to energy production and use. It is also worth noticing that the catalyst use was only considered for five consecutive times in total (i.e., reuse for four runs), in accordance with reusability data in Section 3.6; however, in a more realistic scenario during the use of magnetic catalysts in industrial applications, this reuse will be performed many times. This will lead to a further reduction of environmental impacts.

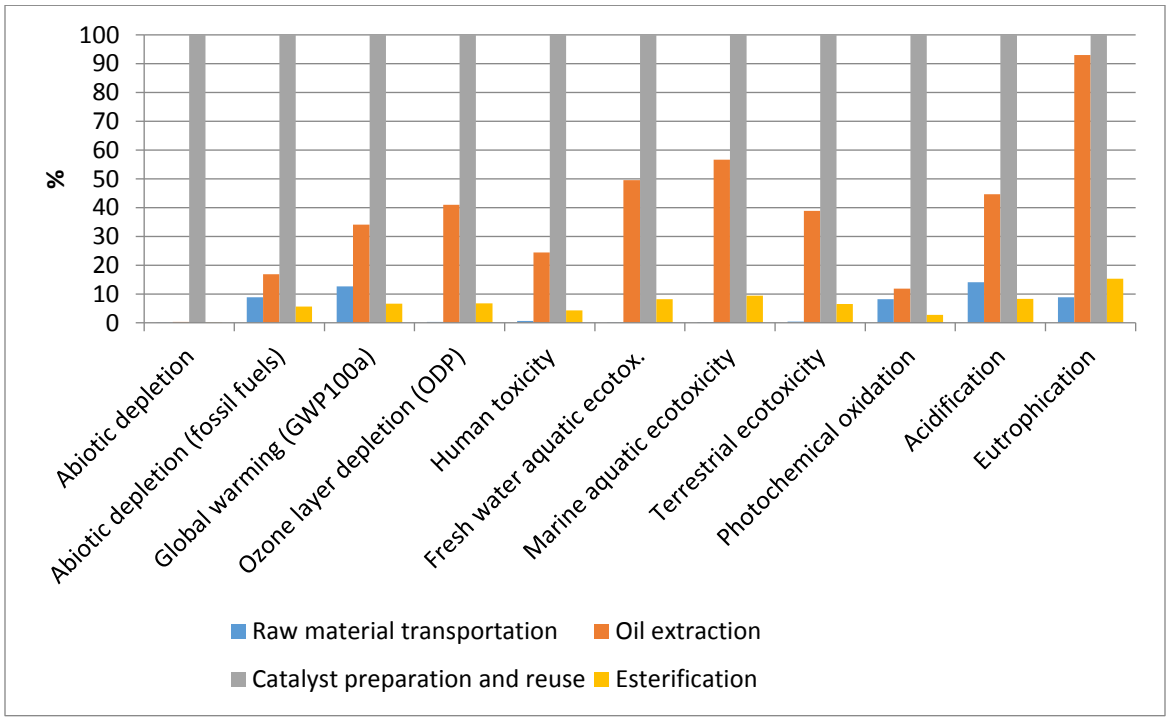


**Figure 10:** CML-IA baseline V3.06 midpoint indicators for 1000 kg of biodiesel production using waste date seed oil.

*[Note: Catalyst reuse was considered for four runs]*

### 3.7.4 Endpoint indicator assessment

ReCiPe 2016 Endpoint (E) V1.04 was used to conduct endpoint analysis. Table 6 shows endpoint indicator assessment for the overall process, including human health, ecosystem quality and resources. Ecosystem quality comprises of acidification, ecotoxicity, eutrophication and land use. Regarding human health, it is related to the impacts of environmental degradation that increases of, and duration of loss-of-life-years related diseases. Whilst for resources, it is closely related to the depletion rate of raw materials and energy sources. Agricultural resource depletion in the form of land-use change is not considered as date seeds do not require plantation due to their source from waste. Results are evaluated based on the future energy surplus requirements needed to produce lower-quality energy and minerals. The findings obtained from the endpoint impact assessment are in accordance with midpoint indicator impact assessment (Table 6), with transportation, being the least contributor to damage to ecosystems and human health.

**Table 6.** Environmental impacts due to biodiesel production process (1000 kg) computed using ReCiPe 2016 Endpoint (E) V1.04.

| Damage category | Unit | Raw material transportation | Oil extraction | Catalyst preparation and [a] reuse | Esterification |
|---|---|---|---|---|---|
| **Human health** | DALY | 0.001 | 0.024 | 0.045 | 0.004 |
| **Ecosystems** | species.yr | $2.4563 \times 10^{-6}$ | $1.513 \times 10^{-5}$ | $3.440 \times 10^{-5}$ | $2.632 \times 10^{-6}$ |
| **Resources** | USD2013 | 12.599 | 11.223 | 117.482 | 4.182 |

*[[a] Catalyst reuse was considered for four runs]*

The cumulative human health, ecosystems and resources impact over the entire process were observed as 330.45 Pt, 25.92 Pt, and 1.04 Pt, respectively (Figure 11). LCA's overall results show that 19037 MJ of energy was required to produce biofuel quantities of 1000 kg (1 functional unit) with a calorific value of 41.39 MJ/kg. Thus, the energy ratio computed using output as 41390 MJ shows an energy ratio of 2.17, which is in close range with the energy ratio for palm oil biodiesel reported by Pleanjai and Gheewala [54] as 3.15. Moreover, 1.11 kg $CO_2$

eq/kg of carbon emissions, took place due to date seed oil biodiesel in the present study, which is comparable with palm oil biodiesel as 1.07 kg $CO_2$ eq/kg. Nevertheless, it should be noted that date seed biodiesel produced in the present study was from a waste-derived feedstock and catalyst was used for a total of five runs. While palm oil is produced using agricultural plantations [54], which leads to drastic environmental concerns due to land-use change. Therefore, the present study demonstrated that even when specific energy crops are not utilised for biodiesel production, the energy ratio and carbon emissions can be comparable.

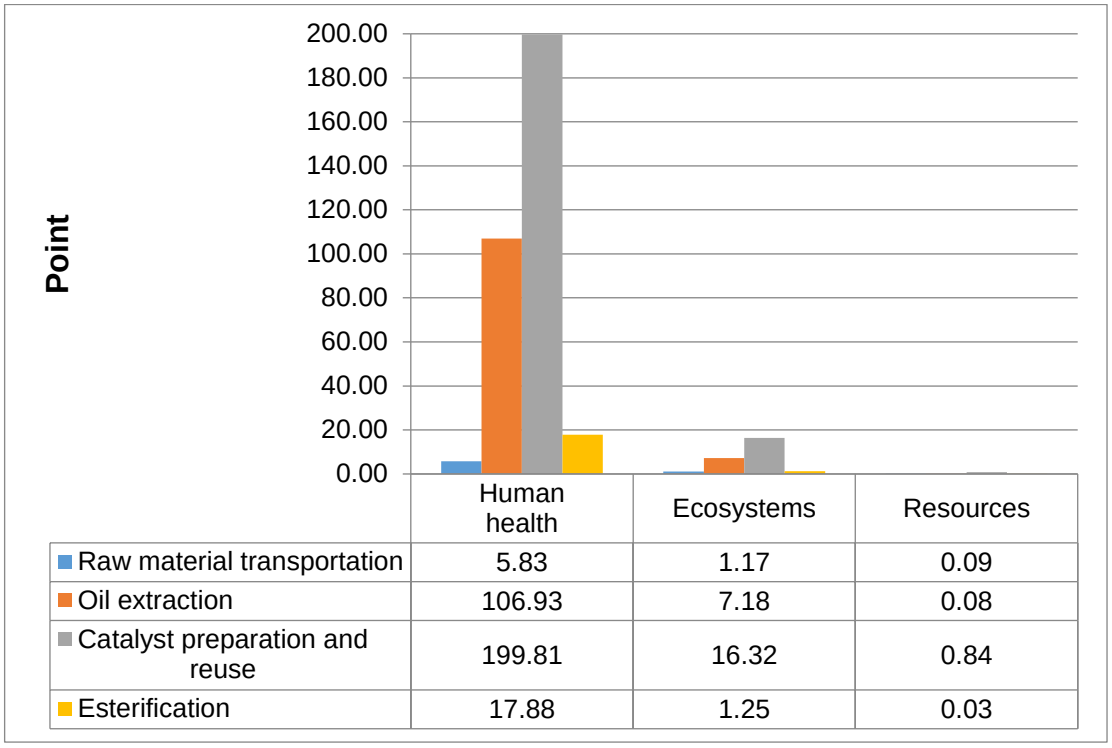


| | Human health | Ecosystems | Resources |
|---|---|---|---|
| Raw material transportation | 5.83 | 1.17 | 0.09 |
| Oil extraction | 106.93 | 7.18 | 0.08 |
| Catalyst preparation and reuse | 199.81 | 16.32 | 0.84 |
| Esterification | 17.88 | 1.25 | 0.03 |

**Figure 11:** ReCiPe 2016 Endpoint (E) V1.04 endpoint indicators for producing 1000 kg of biodiesel using date seed oil.

*[Note: Catalyst reuse was considered for four runs]*

## 4. Conclusion

Upcycling biomass waste into sustainable energy sources following a circular bioeconomy approach has two-fold benefits: (1) mitigation of waste management issues; and (2) to provide renewable energy sources. Biodiesel production through transesterification needs a specific acid value of bio-oil to increase the biodiesel yield, so an acidic heterogeneous catalyst was synthesised and used for converting the free fatty acids contained in the waste date seed oil into biodiesel. The mercaptoacetic acid supported on iron oxide nanoparticles was used as a magnetic solid acid catalyst herein. The esterification reaction was optimised by considering the temperature, time and catalyst loading to increase the percentage of FFAs conversion (biodiesel yield). The optimised FFAs conversion was 90 % when the temperature was 55 °C, time 47 min., and catalyst loading 1.5 wt.% of pretreated oil. Statistical analysis ANOVA was also used, which indicated that the suggested mathematical model was in good agreement with experimental data. The significance of the model was checked from its p-value, less than 0.05, which shows its significance. Furthermore, the FFA conversion (biodiesel yield) calculated using the predicted model was in good agreement with the actual yield obtained from experiments.

The LCA results by using midpoint indicators for 1000 kg of biodiesel production (1 Functional unit) showed the cumulative abiotic depletion of fossil resources over all the processes as 18740.2 MJ, global warming potential as 1084.13 kg $CO_2$ eq, and human health toxicity as 618.45 kg 1,4-DB eq (kg 1,4 dichlorobenzene eq). The highest damage in all categories was observed during catalyst preparation and reuse for four runs. This was confirmed in endpoint LCA findings (ReCiPe 2016 Endpoint (E) V1.04), where catalyst preparation and reuse for four runs contributed impacts to human health (199.81 Pt), ecosystems damage (16.32 Pt) and resources depletion (0.84 Pt). The cumulative human health, ecosystems and resources impact

over the entire process were observed as 330.45 Pt, 25.92 Pt, and 1.04 Pt respectively. The energy ratio for the entire process was computed as 2.17 and carbon emissions as 1.11 kg $CO_2$ eq/kg.

The utilisation of waste date seeds in biodiesel production helps address the growth of the circular bioeconomy by upcycling an otherwise waste and problematic thermochemical conversion feedstock by adding value and providing potential routes for application in the energy sector.

**Acknowledgment:**

The authors would like to thank Sultan Qaboos University and the College of Engineering for their support during this work. Ahmed Osman and David Rooney would like to acknowledge the support given by the EPSRC project "Advancing Creative Circular Economies for Plastics via Technological-Social Transitions" (ACCEPT Transitions, EP/S025545/1) and the support of The Bryden Centre project (Project ID VA5048) which was awarded by The European Union's INTERREG VA Programme, managed by the Special EU Programmes Body (SEUPB), with match funding provided by the Department for the Economy in Northern Ireland and the Department of Business, Enterprise and Innovation in the Republic of Ireland.

**Disclaimer**

The views and opinions expressed in this paper do not necessarily reflect those of the European Commission or the Special EU Programmes Body (SEUPB).

**Competing interests:** The authors declare no competing interests.

**Uncategorized References**


[1] P. Stegmann, M. Londo, M. Junginger, The circular bioeconomy: Its elements and role in European bioeconomy clusters, Resources, Conservation & Recycling: X 6 (2020) 100029.

[2] Konstantinos P. Tsagarakis, Ioannis Nikolaou, F. Konstantakopoulou, Circular Economy, Ethical Funds, and Engineering Projects, https://doi.org/10.3390/books978-3-03928-253-1, Sustainability ISBN 978-3-03928-252-4 (Pbk); ISBN 978-3-03928-253-1 (PDF) (2020) 1-300.

[3] M.A. Amani, M.S. Davoudi, K. Tahvildari, S.M. Nabavi, M.S. Davoudi, Biodiesel production from Phoenix dactylifera as a new feedstock, Industrial Crops and Products 43 (2013) 40-43.

[4] M.W. Azeem, M.A. Hanif, J.N. Al-Sabahi, A.A. Khan, S. Naz, A. Ijaz, Production of biodiesel from low priced, renewable and abundant date seed oil, Renewable energy 86 (2016) 124-132.

[5] K. Krisnangkura, A simple method for estimation of cetane index of vegetable oil methyl esters, Journal of the American Oil Chemists' Society 63(4) (1986) 552-553.

[6] L. Meher, D.V. Sagar, S. Naik, Technical aspects of biodiesel production by transesterification—a review, Renewable and sustainable energy reviews 10(3) (2006) 248-268.

[7] F. Ma, M.A. Hanna, Biodiesel production: a review, Bioresource technology 70(1) (1999) 1-15.

[8] S. Pasias, N. Barakos, C. Alexopoulos, N. Papayannakos, Heterogeneously catalyzed esterification of FFAs in vegetable oils, Chemical Engineering & Technology: Industrial Chemistry-Plant Equipment-Process Engineering-Biotechnology 29(11) (2006) 1365-1371.

[9] S. Fawzy, A.I. Osman, J. Doran, D.W. Rooney, Strategies for mitigation of climate change: a review, Environmental Chemistry Letters 18(6) (2020) 2069-2094.

[10] A.I. Osman, M. Hefny, M.I.A. Abdel Maksoud, A.M. Elgarahy, D.W. Rooney, Recent advances in carbon capture storage and utilisation technologies: a review, Environmental Chemistry Letters (2020).

[11] L. Lin, Z. Cunshan, S. Vittayapadung, S. Xiangqian, D. Mingdong, Opportunities and challenges for biodiesel fuel, Applied energy 88(4) (2011) 1020-1031.

[12] M.A. Al-Farsi, C.Y. Lee, Optimization of phenolics and dietary fibre extraction from date seeds, Food Chemistry 108(3) (2008) 977-985.

[13] S. Besbes, C. Blecker, C. Deroanne, G. Lognay, N.-E. Drira, H. Attia, Heating effects on some quality characteristics of date seed oil, Food chemistry 91(3) (2005) 469-476.

[14] F. Jamil, Valorization of Omani waste Date (Phoenix Dactylifera) pits for production of biofuels Petroleum and Chemical Engineering Sultan Qaboos University Sultanate of Oman 2017, p. 254.

[15] A.T. Madsen, R. Fehrmann, Catalytic Production of Biodiesel, Centre for Catalysis and Sustainable Chemistry (2011).

[16] A.M. Abu-Jrai, F. Jamil, H. Ala'a, M. Baawain, L. Al-Haj, M. Al-Hinai, M. Al-Abri, S. Rafiq, Valorization of waste Date pits biomass for biodiesel production in presence of green carbon catalyst, Energy Conversion and Management 135 (2017) 236-243.

[17] E. Lotero, Y. Liu, D.E. Lopez, K. Suwannakarn, D.A. Bruce, J.G. Goodwin, Synthesis of biodiesel via acid catalysis, Industrial & engineering chemistry research 44(14) (2005) 5353-5363.

[18] S. Steinigeweg, J. Gmehling, Esterification of a fatty acid by reactive distillation, Industrial & Engineering Chemistry Research 42(15) (2003) 3612-3619.

[19] G.G. Kombe, Chemical modification of high free fatty acid oils for biodiesel production, Fatty Acids, Elsevier2017, pp. 305-327.

[20] S. Shanmugam, B. Viswanathan, T. Varadarajan, Esterification by solid acid catalysts—a comparison, Journal of Molecular Catalysis A: Chemical 223(1-2) (2004) 143-147.

[21] A.I. Osman, N.C. Skillen, P.K.J. Robertson, D.W. Rooney, K. Morgan, Exploring the photocatalytic hydrogen production potential of titania doped with alumina derived from foil waste, International Journal of Hydrogen Energy (2020).

[22] M. Cîrcu, A. Nan, G. Borodi, J. Liebscher, R. Turcu, Refinement of magnetite nanoparticles by coating with organic stabilizers, Nanomaterials 6(12) (2016) 228.
[23] M.I.A. Abdel Maksoud, A.M. Elgarahy, C. Farrell, A.a.H. Al-Muhtaseb, D.W. Rooney, A.I. Osman, Insight on water remediation application using magnetic nanomaterials and biosorbents, Coordination Chemistry Reviews 403 (2020) Article number 213096, (1-33).
[24] M. Mahmoudi, H. Hofmann, B. Rothen-Rutishauser, A. Petri-Fink, Assessing the in vitro and in vivo toxicity of superparamagnetic iron oxide nanoparticles, Chemical reviews 112(4) (2011) 2323-2338.
[25] A.H. Lu, E.e.L. Salabas, F. Schüth, Magnetic nanoparticles: synthesis, protection, functionalization, and application, Angewandte Chemie International Edition 46(8) (2007) 1222-1244.
[26] M. Calero, L. Gutiérrez, G. Salas, Y. Luengo, A. Lázaro, P. Acedo, M.P. Morales, R. Miranda, A. Villanueva, Efficient and safe internalization of magnetic iron oxide nanoparticles: two fundamental requirements for biomedical applications, Nanomedicine: Nanotechnology, Biology and Medicine 10(4) (2014) 733-743.
[27] M. Kazemi, A. Dadkhah, Antioxidant activity of date seed oils of fifteen varieties from iran, Orient J Chem 28(3) (2012) 1201-5.
[28] ISO. ISO 14044 Environmental Management. Life Cycle Assessment. Requirements and Guidelines. Int. Organ. Stand. 1, 1–46., (2006).
[29] I.A. Nehdi, H.M. Sbihi, S. Mokbli, U. Rashid, S.I. Al-Resayes, Yucca aloifolia oil methyl esters, Industrial Crops and Products 69 (2015) 257-262.
[30] A. Karmakar, S. Karmakar, S. Mukherjee, Properties of various plants and animals feedstocks for biodiesel production, Bioresource technology 101(19) (2010) 7201-7210.
[31] G. Knothe, R.O. Dunn, M.O. Bagby, Biodiesel: the use of vegetable oils and their derivatives as alternative diesel fuels, ACS symposium series, Washington, DC: American Chemical Society,[1974]-, 1997, pp. 172-208.
[32] U. Rashid, H.A. Rehman, I. Hussain, M. Ibrahim, M.S. Haider, Muskmelon (Cucumis melo) seed oil: A potential non-food oil source for biodiesel production, Energy 36(9) (2011) 5632-5639.
[33] U. Rashid, F. Anwar, M. Ashraf, M. Saleem, S. Yusup, Application of response surface methodology for optimizing transesterification of Moringa oleifera oil: Biodiesel production, Energy Conversion and Management 52(8-9) (2011) 3034-3042.
[34] R. Dutta, U. Sarkar, A. Mukherjee, Extraction of oil from Crotalaria Juncea seeds in a modified Soxhlet apparatus: physical and chemical characterization of a prospective bio-fuel, Fuel 116 (2014) 794-802.
[35] M. Farooq, A. Ramli, D. Subbarao, Biodiesel production from waste cooking oil using bifunctional heterogeneous solid catalysts, Journal of Cleaner Production 59 (2013) 131-140.
[36] W. Wu, Z. Wu, T. Yu, C. Jiang, W.-S. Kim, Recent progress on magnetic iron oxide nanoparticles: synthesis, surface functional strategies and biomedical applications, Science and technology of advanced materials 16(2) (2015) 023501.
[37] G. Demazeau, Solvothermal reactions: an original route for the synthesis of novel materials, Journal of Materials Science 43(7) (2008) 2104-2114.
[38] Q. Lan, C. Liu, F. Yang, S. Liu, J. Xu, D. Sun, Synthesis of bilayer oleic acid-coated Fe3O4 nanoparticles and their application in pH-responsive Pickering emulsions, Journal of colloid and interface science 310(1) (2007) 260-269.
[39] S. Pereira da Silva, D. Costa de Moraes, D. Samios, Iron Oxide Nanoparticles Coated with Polymer Derived from Epoxidized Oleic Acid and Cis-1, 2-Cyclohexanedicarboxylic Anhydride: Synthesis and Characterization, J Material Sci Eng 5(247) (2016) 2169-0022.1000247.
[40] M. Bloemen, W. Brullot, T.T. Luong, N. Geukens, A. Gils, T. Verbiest, Improved functionalization of oleic acid-coated iron oxide nanoparticles for biomedical applications, Journal of Nanoparticle Research 14(9) (2012) 1100.

[41] M. Chai, Q. Tu, M. Lu, Y.J. Yang, Esterification pretreatment of free fatty acid in biodiesel production, from laboratory to industry, Fuel processing technology 125 (2014) 106-113.
[42] W. Visser, J.-M. Hoc, Expert software design strategies, Psychology of programming, Elsevier1990, pp. 235-249.
[43] A. Hooda, A. Nanda, M. Jain, V. Kumar, P. Rathee, Optimization and evaluation of gastroretentive ranitidine HCl microspheres by using design expert software, International journal of biological macromolecules 51(5) (2012) 691-700.
[44] ISO, ISO 14040: *Environmental Management—Life Cycle Assessment— Principles and Framework*; Technical Committee ISO/TC 207; ISO: Geneva, Switzerland. Int. Organ. Stand. 3, 1–20., (2006).
[45] A. Fridrihsone, F. Romagnoli, U. Cabulis, Environmental Life Cycle Assessment of Rapeseed and Rapeseed Oil Produced in Northern Europe: A Latvian Case Study, Sustainability 12(14) (2020) 5699.
[46] S. Photaworn, C. Tongurai, S. Kungsanunt, Process development of two-step esterification plus catalyst solution recycling on waste vegetable oil possessing high free fatty acid, Chemical Engineering and Processing: Process Intensification 118 (2017) 1-8.
[47] W. Marimón-Bolívar, E.E. González, Green synthesis with enhanced magnetization and life cycle assessment of Fe3O4 nanoparticles, Environmental Nanotechnology, Monitoring & Management 9 (2018) 58-66.
[48] J. Dufour, D. Iribarren, Life cycle assessment of biodiesel production from free fatty acid-rich wastes, Renewable Energy 38(1) (2012) 155-162.
[49] G. Barjoveanu, O.-A. Pătrăuțanu, C. Teodosiu, I. Volf, Life cycle assessment of polyphenols extraction processes from waste biomass, Scientific Reports 10(1) (2020) 13632.
[50] Energy for oven drying. Available at: Grinder. Grinder properties. Available at: https://www.alibaba.com/product-detail/small-dry-date-seed-powder-grinder_60783543495.html?spm=a2700.7724857.0.0.547848825gOcaQ.
[51] Energy for oilseeds cooking machine. Available at: https://oil-mill-plant.com/oilseeds-preprocessing-machines/oilseed-cooker.html.
[52] Energy for flaker roll. Available at: https://www.alibaba.com/product-detail/Automatic-Flaker-Roll-Soybean-Sunflower-Peanut_60825427350.html?spm=a2700.pc_countrysearch.main07.3.65122ef7wnDRym.
[53] Z.L. Chung, Y.H. Tan, Y.S. Chan, J. Kansedo, N.M. Mubarak, M. Ghasemi, M.O. Abdullah, Life cycle assessment of waste cooking oil for biodiesel production using waste chicken eggshell derived CaO as catalyst via transesterification, Biocatalysis and Agricultural Biotechnology 21 (2019) 101317.
[54] S. Pleanjai, S.H. Gheewala, Full chain energy analysis of biodiesel production from palm oil in Thailand, Applied Energy 86 (2009) S209-S214.